SUPPLEMENTAL MATERIAL

TGF-β signaling promotes pulmonary hypertension caused by *Schistosoma mansoni*

Supplemental Methods

Animals

All mice were bred and housed under specific pathogen-free conditions in an American Association for the Accreditation of Laboratory Animal Care-approved facility. All experiments were performed in a coded format, with the investigators lacking knowledge of the specific experimental group identifiers prior to final data reporting. Bone marrow recipients were maintained on diet containing trimethoprim-sulfa antibiotic for 4 weeks after transplant, but otherwise all mice were maintained on normal rodent diet.

Bone Marrow Transplantation

For bone marrow transplantation, recipient mice were irradiated with 10 Gy split in 2 fractions, delivered 4 hours apart, and 0.5-2.0x10^6 bone marrow cells isolated from the thigh of donor mice were administered by tail vein injection shortly thereafter; mice were allowed to recover for at least 8 weeks before undergoing additional treatments as described above.

Assessment of Oxygen Saturation

Pimonidazole hydrochloride (Hypoxyprobe; HPI Inc., Burlington, MA) was purchased and a single 60µg/g dose administered IP 2 hours before sacrifice. Oxygen saturation was measured non-invasively in non-sedated mice by tail probe (MouseOx, Starr Life Sciences, Pittsburgh, PA).

Egg Burden Quantification

The number of *S. mansoni* ova present in mouse lung tissue was determined as previously described (1). Briefly, 10 to 20 mg of frozen right lung tissue was digested in 4% potassium hydroxide for 18 hours at 33degC, and the number of eggs in aliquots of the digest was counted.

Protein and RNA Assessment

After the right ventricular catheterization was complete, the blood was flushed out of the lungs, the right bronchus sutured, and 2% agarose instilled into the left lung through the transtracheal catheter. The left lung was removed, formalin-fixed, and processed for paraffin embedding. The right lung was removed and divided into lobes which were frozen or placed in RNAlater (Life Technologies, Carlsbad, CA). The right ventricle free wall was dissected off of the heart, weighed relative to the septum and left ventricle, and formalin-fixed and paraffin-embedded.

A sample of the right lung frozen tissue was macerated and sonicated in PBS containing anti-proteases, protein concentration determined by Bradford assay (BioRad), and 50 µg of protein from each sample was used to detect specific proteins by Western blot using the reagents listed in the Supplemental Table 3. ELISA, including GLISA for GTP-RhoA, was performed to determine the concentration of specific proteins in samples using the kits in Supplemental Table 4. mRNA expression levels quantified using an Illumina (San Diego, CA) HiSeq 2000 RNA sequencing (RNA-seq) system were expressed as reads per kilobase of exon model per million mapped reads (RPKM: the Illumina standard).

Image Analysis

Images were acquired using a Nikon Eclipse E800 microscope with 10x, 20x and 40x air objectives, at room temperature, using either a color camera (Nikon, Melville, NY) or a black and white CCD camera (Photometrics, Tuscon, AZ), with Nikon NIS Elements Software v3.2. Quantification of media and intima thickness in mouse lung tissue was determined as previously described (2). Briefly, 10 to 12 images of vessels at 40x magnification were randomly acquired from masked paraffin-embedded samples immunofluorescence stained for α–smooth muscle actin and thrombomodulin, or smooth muscle myosin heavy chain, as described above. Image

processing software (Image Pro Plus v4.5.1, Media Cybernetics, Bethesda, MD) was used to identify the cross-sectional areas contained by the external perimeter of the media, the internal perimeter of the media, and the internal perimeter of the intima. The radius r_i for each of the three vessel layers i enclosing an area A_i was calculated using the equation $r_i = \sqrt{A_i/\pi}$. The thicknesses of the media and intima were calculated as the differences between the respective radii, and expressed as a fraction of the external media radius. Peri-egg granuloma volumes were measured using the optical rotator sterologic method (3). Briefly, paraffin-embedded tissue was stained with hematoxalin and eosin, and 8-10 images of granulomas with a single visible ova were acquired for each sample. The rotator method for object volume estimation was then applied using the ova as the central reference point with image processing software (Image Pro Plus). Co-localization and pixel intensity analysis of Mac3 with TGF-β1 and pSmad2/3 with α–smooth muscle actin and thrombomodulin was performed by acquiring 10 to 12 images of vessels, parenchyma and granulomas from each sample. Image processing software (Metamorph, Molecular Devices LLC, Sunnyvale, CA) was used to threshold each signal for positive cells, and the area occupied by the thresholded area for each signal (and co-localized areas) as well as the average pixel intensity within thresholded areas was determined; the adventitia was taken as the space outside the media and inside twice the diameter of the external media layer. Picrosirius red was used to quantify right ventricular fibrosis in unexposed and IP/IV egg-exposed mice. Ten images of each mouse were acquired at 10x magnification and superimposed on a 1700 point grid using MetaMorph software. Points intersecting with collagen (positive polarization with picrosirius red staining) were counted and used to determine the volume fraction of RV free wall fibrosis. 10 images of fluorescein-labeled wheat germ agglutinin-stained (see above) RV free wall tissue were acquired at 40x magnification. These images were analyzed using MetaMorph to determine the volume density of myocytes (using the same point intersection as for picrosirius red staining above) and myocyte cross sectional

area. To exclude longitudinally sectioned myocytes, a length to breadth ratio of 2:1 was implemented. Likewise, a size exclusion selected myocyte area between 30μm and 550μm for quantification.

Supplemental Tables

Table S1. Reagents for immunostaining mouse tissue.

Immunostain	Antigen Retrieval	Block	Primary Antibody	Secondary Antibody	Tertiary Reagent
Hexokinase	Citrate Buffer 30 min in steamer (Vector H-3300)	Peroxidase block (Dako S2003) 10min at RT, 3% H2O2 10min at RTx3 each, Avidin 10 min, Biotin 10 min, 1.5% Goat Serum in PBS	1:50 30min at RT (Cell Signaling #2106)	1:200 Biotinylated Goat anti-Rabbit (Vector BA1000) 1hr at RT	Strepavidin-HRP (Vector #SA-5704), then DAB 5min, then Hematoxalyn
GLUT1			1:100 1hr at RT (Thermo Scientific #RB-9052)		
Hypoxyprobe		Serum free protein block (Dako X0909)	1:50 40min at RT (MAb1, HPI Inc.)	1:200 Biotinylated Goat anti-Mouse (Dako E0464)	
TGF-β1		10% Goat Serum in PBS	1:25 O/N at 4degC (R&D Systems AF-101-NA)	AF488 Goat anti-Chicken IgY (Invitrogen A11039)	Vectashield with DAPI (Vector H-1200)
BrdU		10% Donkey Serum in PBS, Avidin 10 min, Biotin 10 min	1:50 O/N at 4degC (Abcam #1893)	1:200 FITC-labeled Donkey anti-Sheep (Abcam ab6896-1)	
Thrombo-modulin (CD141)		10% Horse Serum in 1:1 5% BSA : Superblock (ScyTek AAA5000) 1hr at RT	1:1000 1hr at RT (R&D Systems #AF3894)	1:200 AF594 Donkey anti-Goat (Invitrogen #A11058) 1hr at RT	
p-Smad2/3		5% Horse Serum in PBS 1hr at RT	1:100 overnight at 4degC (Cell Signaling #3101)	1:100 AF488 Donkey anti-Rabbit (Invitrogen #A21206) 1hr at RT	

Table S1 (continued). Reagents for immunostaining mouse tissue.

Immunostain	Antigen Retrieval	Block	Primary Antibody	Secondary Antibody	Tertiary Reagent
αSM-actin	Citrate Buffer 30 min in steamer (Vector H-3300)	Avidin 10 min, Biotin 10 min, Mouse on Mouse (MOM) kit blocking solution (Vector BMK-2202) 1hr at RT	1:100 30min at RT (Dako #M0851)	MOM Biotinylated anti-Mouse Reagent (Vector BMK-2202) 10min at RT	Texas Red-Strepavidin 1:2000 (Invitrogen #S872), Vectashield with DAPI (Vector H-1200)
Smooth Muscle Myosin Heavy Chain		10% Goat Serum in PBS	1:100 O/N at 4degC (Biomedical Technologies #5620305)	1:200 Texas Red-Goat anti-Rabbit (Invitrogen #T2767) 1hr at RT	Vectashield with DAPI (Vector H-1200)
Mac-3	Borg Buffer 30 min in steamer (Biocare #BD1000G1)	10% Goat Serum in 1:1 5% BSA: Superblock (ScyTek AAA5000) 1hr at RT	1:50 1hr at RT (BD Pharmingen #550292)	1:300 AF488 Goat anti-Rat (Invitrogen #A11006) 1hr at RT	Vectashield with DAPI (Vector H-1200)
Fluorescein-Labeled Wheat Germ Agglutinin	Citrate Buffer 20 min in steamer (Vector H-3300)	None	1:500 O/N at 4degC (Vector FL-1021)	None	Vectashield with DAPI (Vector H-1200)
Picrosirius Red	0.1% (w/v) Sirius red (Direct Red 80, Sigma #365548) in saturated aqueous solution of picric acid, 1hr at RT, followed by 2 rinses of 0.5% acetic acid				

Table S2. Reagents for immunostaining human tissue.

Immunostain	Antigen Retrieval	Block	Primary Antibody	Secondary Antibody	Tertiary Reagent
Hexokinase	Citrate Buffer 30 min in steamer (Vector H-3300)	Peroxidase block (Dako S2003) 10min at RT, 3% H2O2 10min at RTx3 each, Avidin 10 min, Biotin 10 min, 1.5% Goat Serum in PBS	1:50 30min at RT (Cell Signaling #2106)	1:200 Biotinylated Goat anti-Rabbit (Vector BA1000) 1hr at RT	Strepavidin-HRP (Vector #SA-5704), then DAB 5min, then Hematox-alyn
GLUT1			1:100 1hr at RT (Thermo Scientific #RB-9052)		
p-Smad2/3	Citrate Buffer 30 min in steamer (Vector H-3300)	5% Horse Serum in PBS 1hr at RT	1:2000 overnight at 4degC (Cell Signaling #3101)	1:100 AF488 Donkey anti-Rabbit (Invitrogen #A21206) 1hr at RT	Vectashield with DAPI (Vector H-1200)
α-SMactin		5% Goat Serum in PBS 1hr at RT	1:200 1hr at RT (Dako #M0851)	1:100 AF594 Goat anti-Mouse (Invitrogen #A11005) 1hr at RT	

Table S3. Reagents for immunoblotting mouse protein.

Immunoblot	Block	Primary Antibody	Secondary Antibody	Tertiary Reagent
RELM-α	StartingBlock 2hr at RT (Thermo Scientific, #37542)	1:50,000 Abcam #39626 O/N at 4degC	HRP-bound Goat anti-Rabbit 1:5000 1hr at RT (Vector PI-1000)	ECL Detection 5min at RT (GE Healthcare, RPN2106)
β-actin		1:20,000 Cell Signaling #4967 O/N at 4degC		

Table S4. Reagents for quantifying mouse protein.

Protein	Kit
IL4	R&D Systems M4000B
IL13	R&D Systems M1300CB
IFN-γ	R&D Systems MIF00
GTP-RhoA	Cytoskeleton Inc. BK124

Supplemental Figures and Figure Legends

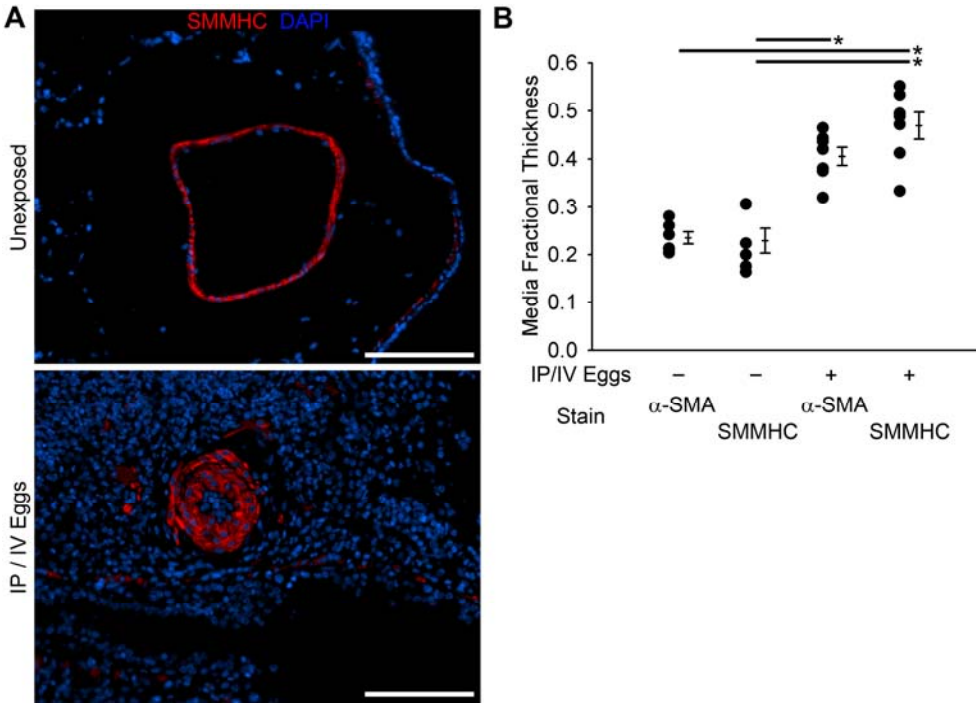

Figure S1.
Antibodies against smooth muscle myosin heavy chain (SMMHC) and α-smooth muscle actin (α-SMA) identify comparable vascular remodeling of the pulmonary media after *S. mansoni* egg exposure. (**A**) Representative immunofluorescence staining for SMMHC of unexposed and IP/IV egg exposed mouse lungs (Scale bars: 100μm). (**B**) Quantitative fractional thickness of the pulmonary vascular media assessed by antibodies against α-SMA and SMMHC in unexposed and IP/IV egg exposed mice (mean ± SE; n = 6-7 mice per group; ANOVA on ranks $P < 0.001$; *P < 0.05 by post-hoc Dunn's test).

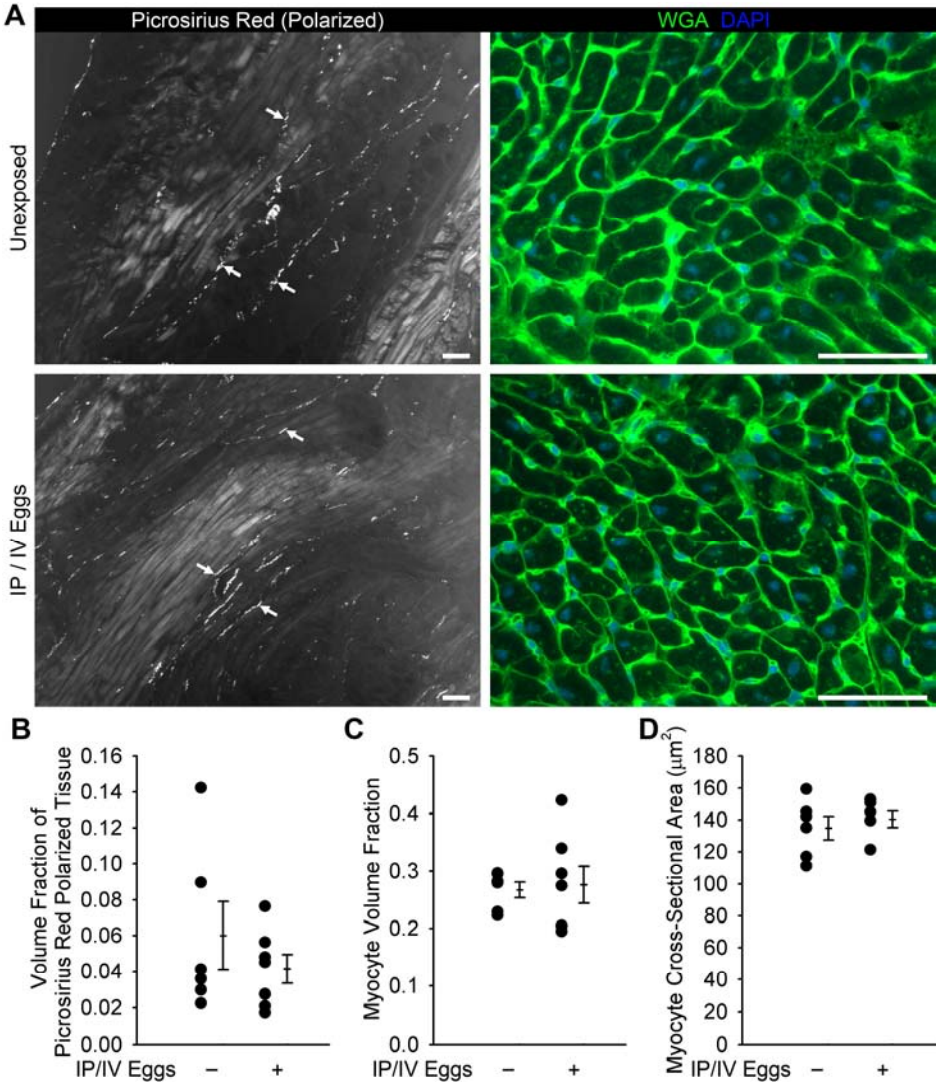

Figure S2.
Exposure to IP/IV *S. mansoni* eggs does not result in RV free wall fibrosis or myocyte hypertrophy. (**A**) Representative picrosirius red and wheat germ agglutin staining to detect fibrosis (picrosirius red stain, imaged using cross-polarized lenses; arrows show areas of fibrosis) and myocyte membranes in the right ventricle of unexposed or IP/IV egg-exposed mice (Scale bars: 50μm). (**B**) Volume fraction of tissue that is polarized positive with picrosirius red stain, related to collagen volume density (see Supplemental Methods, mean ± SE; n = 6-7 mice per group; rank-sum test *P*=0.63). (**C**) Volume fraction of myocytes (see Supplemental Methods, mean ± SE; n = 6-7 mice per group; rank-sum test *P*=0.84). (**D**) Average myocyte cross-sectional area (mean ± SE; n = 6-7 mice per group; rank-sum test *P*=0.53).

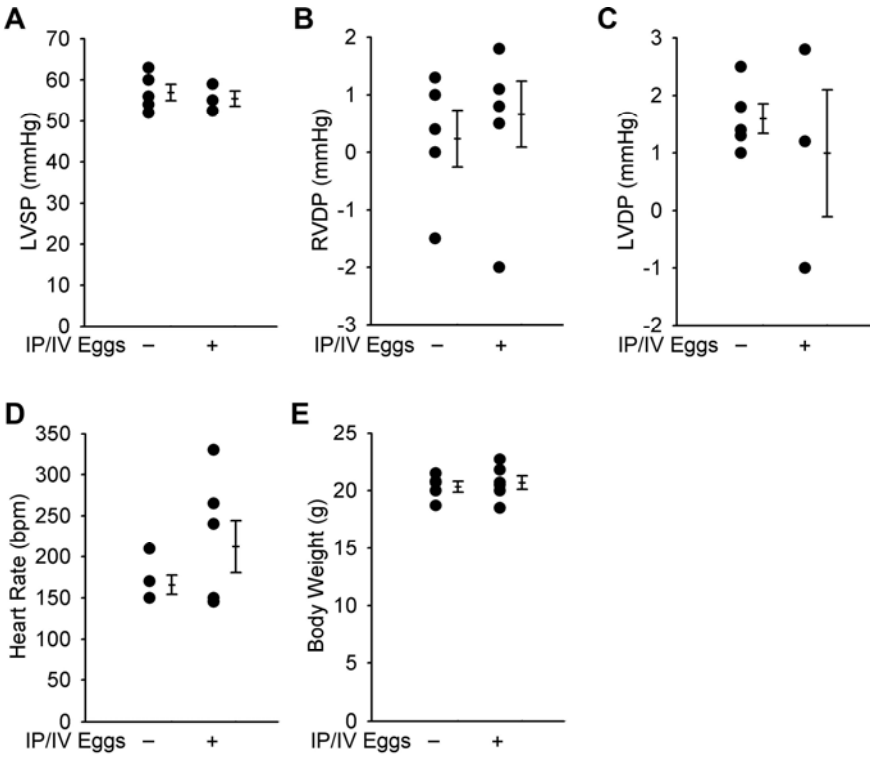

Figure S3.
Exposure to IP/IV *S. mansoni* eggs does not affect systemic hemodynamics or body weight. (**A**) Left ventricular systolic pressure (mean ± SE; n = 3-5 mice per group; rank-sum test *P*=0.79). (**B**) Right ventricular diastolic pressure (mean ± SE; n = 5-6 mice per group; rank-sum test *P*=0.43). (**C**) Right ventricular diastolic pressure (mean ± SE; n = 3-5 mice per group; rank sum test *P*=0.79). (**D**) Heart rate (mean ± SE; n = 5-6 mice per group; rank-sum test *P*=0.80). (**E**) Body weight (mean ± SE; n = 5-6 mice per group; rank-sum test *P*=0.93).

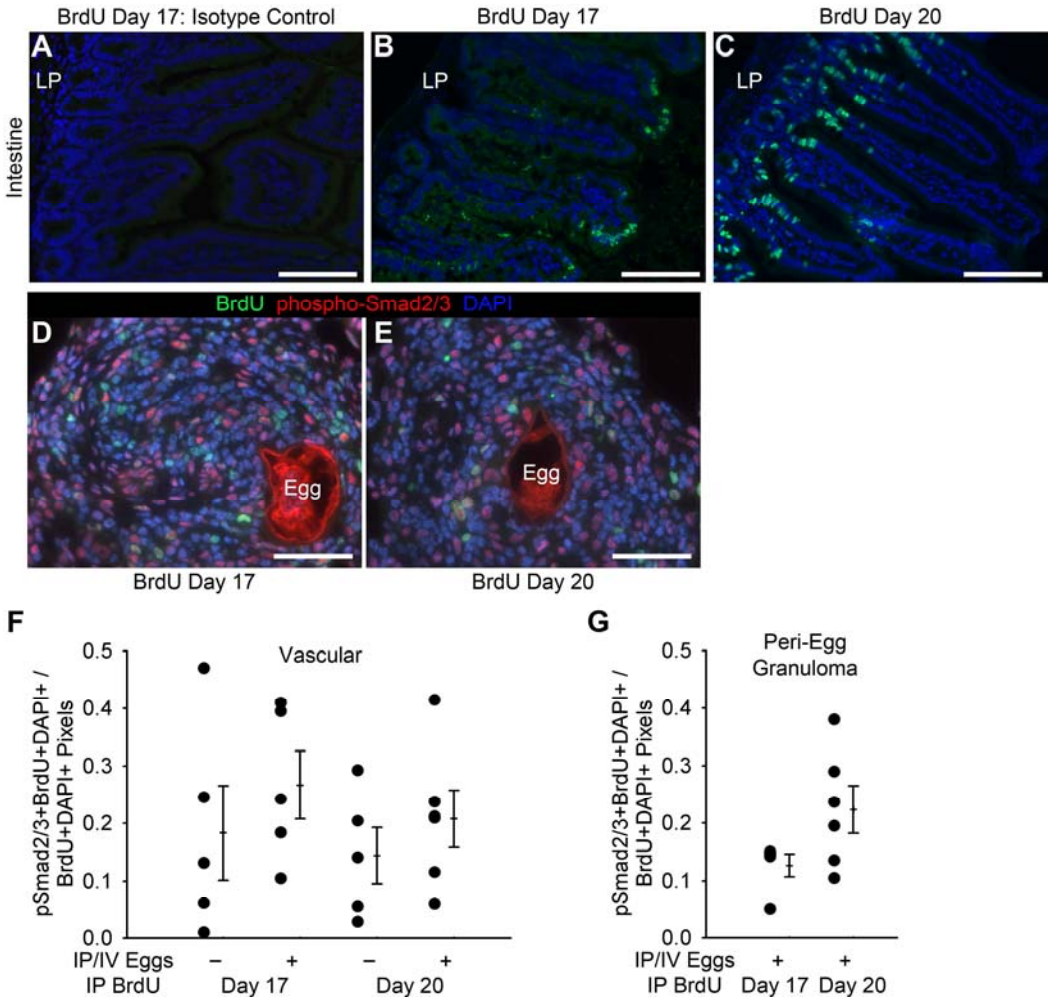

Figure S4.
Additional images of BrdU-treated and GFP bone marrow-recipient mice. (**A**-**C**) Intestine of mice treated with BrdU (**A** is stained with isotype control antibody; LP: lamina propria; Scale bars: 100 μm). (**D** and **E**) Peri-egg granulomas in BrdU-treated *S. mansoni* egg IP/IV exposed mice co-stained for BrdU and phospho-Smad2/3 (Egg: *S. mansoni* egg; Scale bars: 50 μm). (**F**) Fraction of BrdU-positive pixels that are also phospho-Smad2/3-positive in vessels (includes all 3 layers: intima, media, and adventitia) in unexposed and *S. mansoni* egg IP/IV exposed mice (mean ± SE; ANOVA on ranks P=0.59). (**G**) Fraction of BrdU-positive pixels that are also phospho-Smad2/3-positive in peri-egg granulomas in *S. mansoni* egg IP/IV exposed mice (mean ± SE; rank-sum test P=0.25).

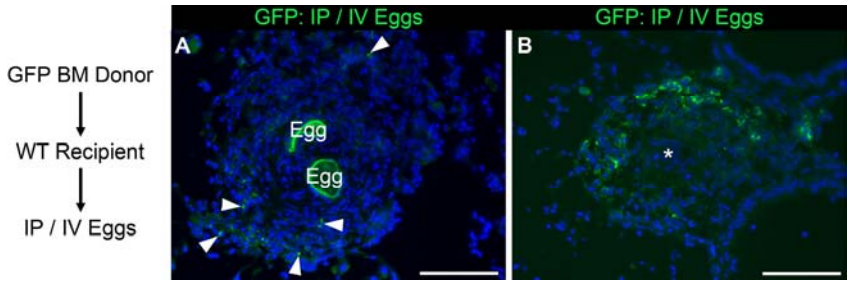

Figure S5.
Additional images of GFP bone marrow-recipient mice. (**A** and **B**) Peri-egg granuloma and peri-vascular GFP signal in wildtype recipient mice with GFP positive bone marrow donor exposed to IP/IV *S. mansoni* eggs (arrowheads mark positive cells; Egg: *S. mansoni* egg; *: vessel lumen; Scale bar: 100 μm; G is the same image as Figure 2G without the dotted lines).

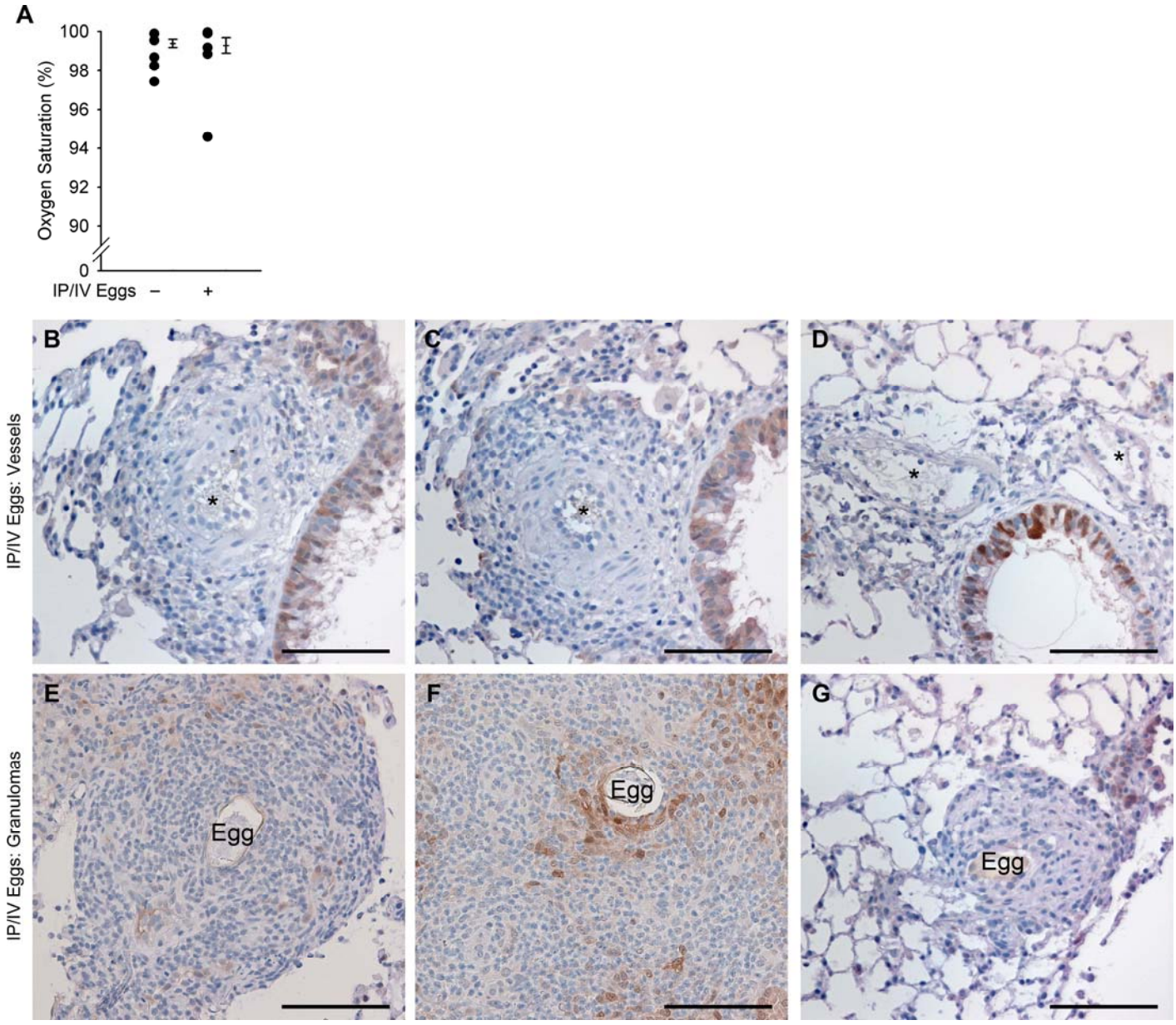

Figure S6.
Absence of significant hypoxia after IP/IV *S. mansoni* egg exposure. (**A**) Non-invasive tail oxygen saturation (mean ± SE; n = 5-6 mice per group; rank-sum test *P*=0.54). (**B**-**D**) Immunostain for pimonazole (hypoxyprobe) of vessels of IP/IV *S. mansoni* egg exposed mice (* vessel lumen; Scale bars: 100 μm). (**E**-**G**) Immunostain for pimonazole (hypoxyprobe) of peri-egg granulomas of IP/IV *S. mansoni* egg exposed mice (Egg: *S. mansoni* egg; Scale bars: 100 μm).

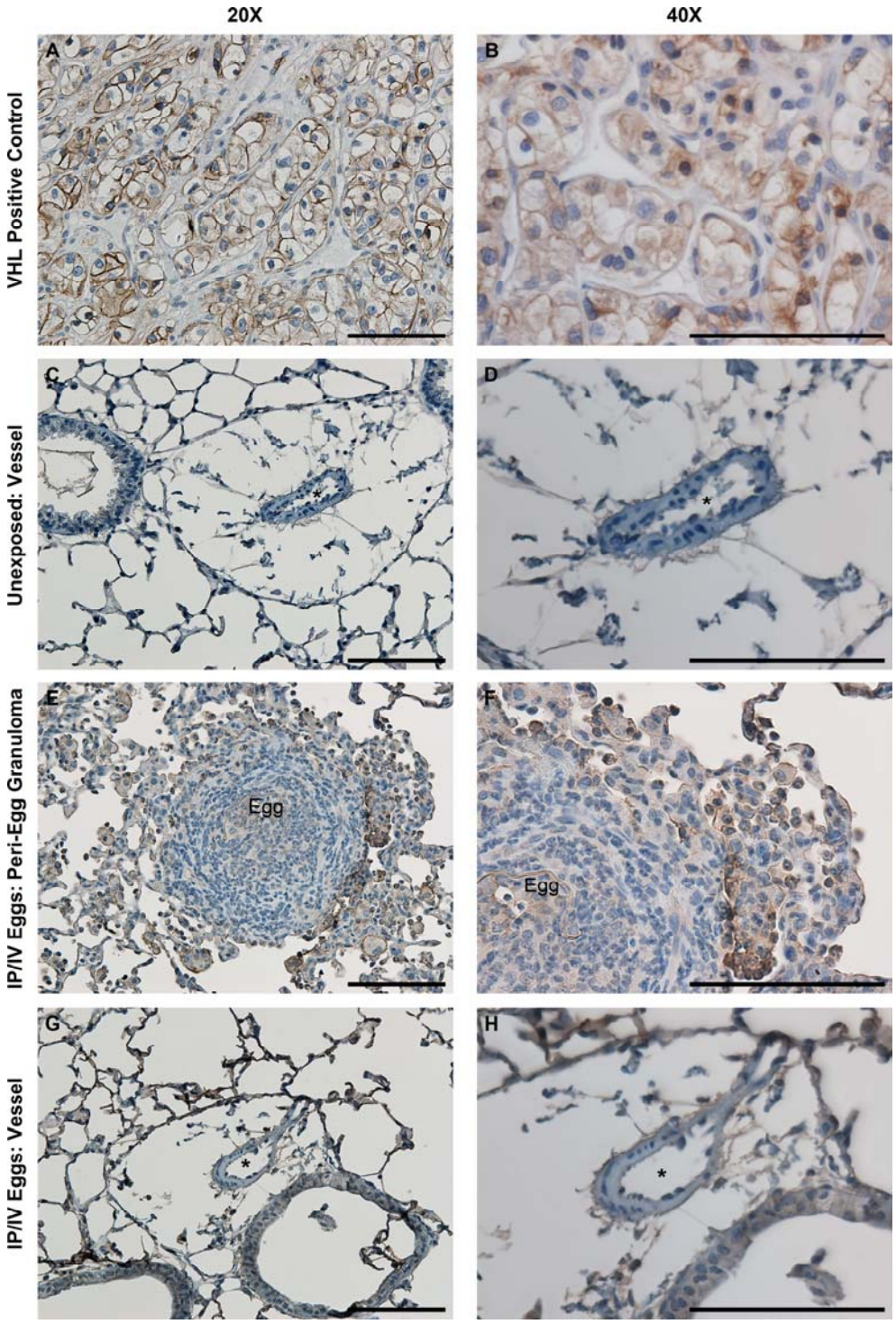

Figure S7.
Immunohistochemistry for glucose transporter 1 (GLUT1) in mouse tissue. (**A** and **B**) Positive control: angiomyolipoma from von Hippel-Lindau disease. (**C** and **D**) Unexposed mouse vessel. (**E** and **F**) Peri-egg granuloma in mice exposed to IP and IV *S. mansoni* eggs. (**G** and **H**) Vessel in mice exposed to IP and IV *S. mansoni* eggs. (* vessel lumen; Egg: *S. mansoni* egg; Scale bars: 100 μm.)

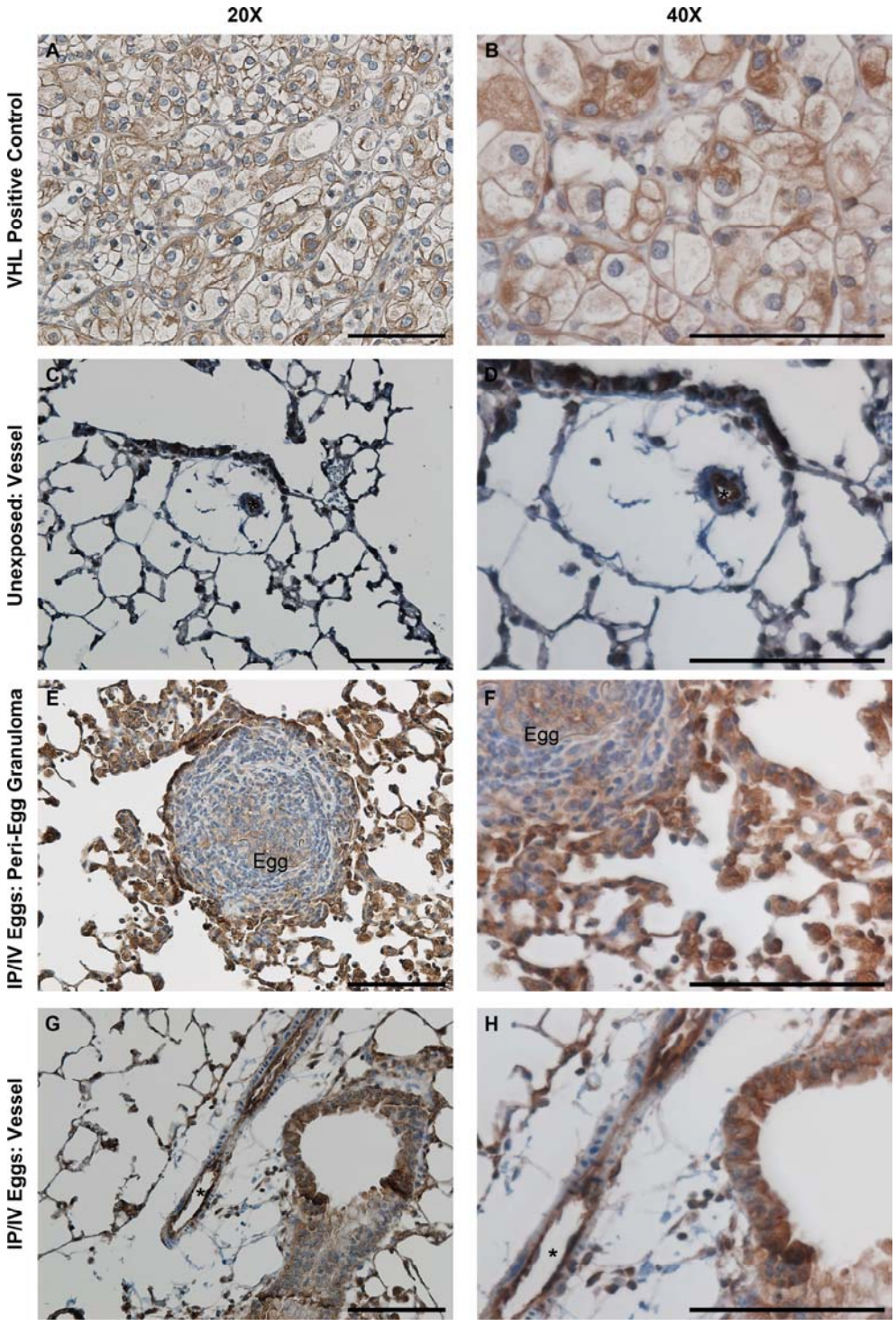

Figure S8.
Immunohistochemistry for hexokinase 2 (HK2) in mouse tissue. (**A** and **B**) Positive control: angiomyolipoma from von Hippel-Lindau disease. (**C** and **D**) Unexposed mouse vessel. (**E** and **F**) Peri-egg granuloma in mice exposed to IP and IV *S. mansoni* eggs. (**G** and **H**) Vessel in mice exposed to IP and IV *S. mansoni* eggs. (* vessel lumen; Egg: *S. mansoni* egg; Scale bars: 100 µm.)

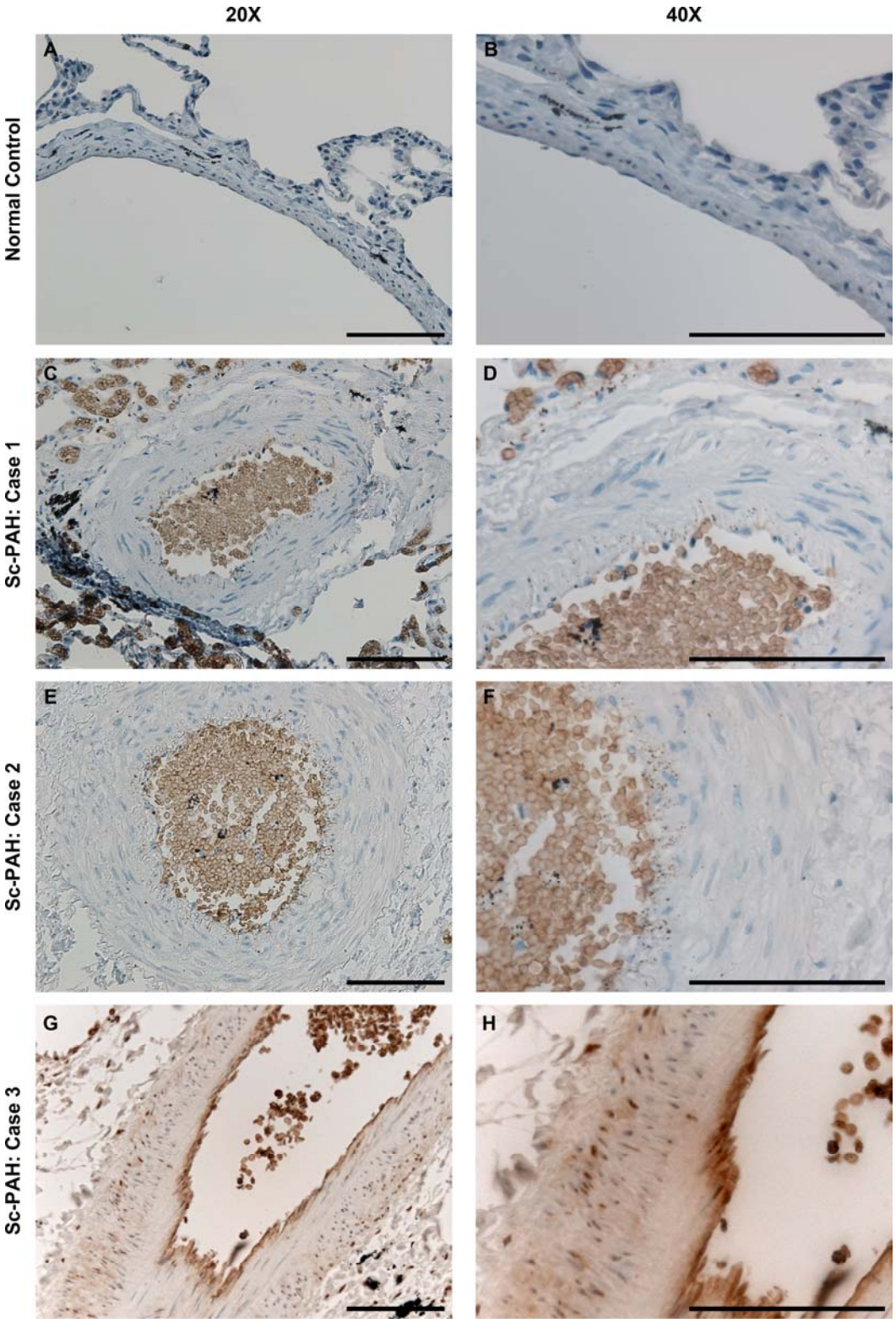

Figure S9.
Immunohistochemistry for glucose transporter 1 (GLUT1) in human tissue. (**A** and **B**) Normal control tissue from a failed lung donor. (**C** - **H**) Lung tissue from three autopsy cases of patients who died of schistosomiasis associated-PAH. (Scale bars: 100 μm.)

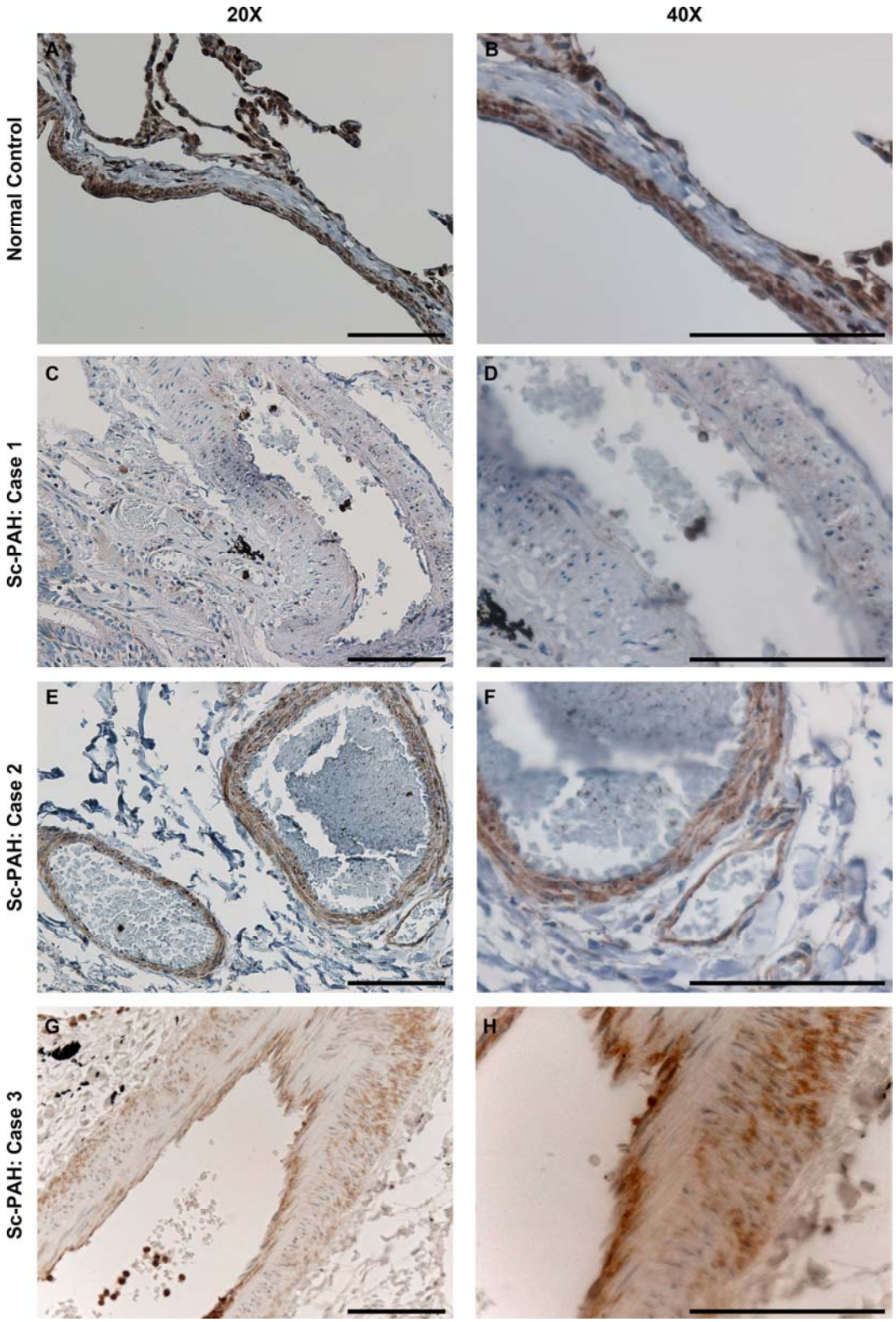

Figure S10.
Immunohistochemistry for hexokinase 2 (HK2) in human tissue. (**A** and **B**) Normal control tissue from a failed lung donor. (**C** - **H**) Lung tissue from three autopsy cases of patients who died of schistosomiasis associated-PAH. (Scale bars: 100 μm.)

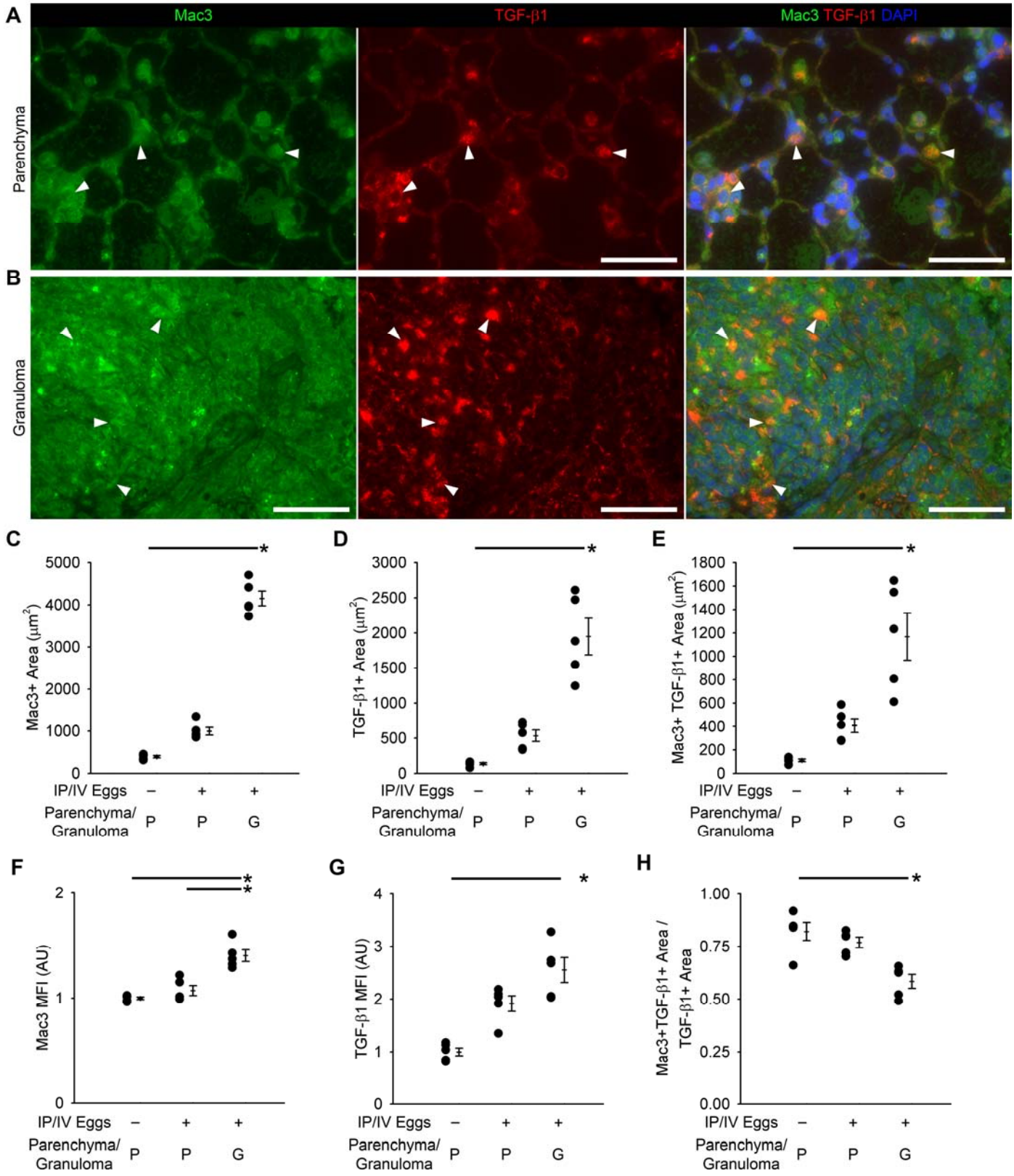
A
Mac3
TGF-β1
Mac3 TGF-β1 DAPI
Parenchyma
B
Granuloma
C
Mac3+ Area (μm²)
D
TGF-β1+ Area (μm²)
E
Mac3+ TGF-β1+ Area (μm²)
IP/IV Eggs
Parenchyma/ Granuloma
F
Mac3 MFI (AU)
G
TGF-β1 MFI (AU)
H
Mac3+TGF-β1+ Area / TGF-β1+ Area

Figure S11.

Quantification of Mac3 (macrophage marker) and TGF-β1 immunostaining and co-localization in the parenchyma and peri-egg granulomas of unexposed and mice exposed to IP and IV *S. mansoni* eggs. (**A** and **B**) Representative images showing Mac3 and TGF-β1 co-localization in the parenchyma and peri-egg granuloma of an IP/IV *S. mansoni* egg-exposed mouse (Scale bars: 50 μm). (**C**) Quantification of Mac3+ area in the parenchyma and peri-egg granulomas (mean ± SE; n = 5 mice per group; ANOVA on ranks P=0.002; *P<0.05 by post-hoc Dunn's test). (**D**) Quantification of TGF-β1+ area in the parenchyma and peri-egg granulomas (mean ± SE; n = 5 mice per group; ANOVA on ranks P=0.002; *P<0.05 by post-hoc Dunn's test). (**E**) Quantification of Mac3+ and TGF-β1+ co-localized area in the parenchyma and peri-egg granulomas (mean ± SE; n = 5 mice per group; ANOVA on ranks P=0.002; *: P<0.05 by post-hoc Dunn's test). (**F**) Mean fluorescent intensity of Mac3+ pixels (arbitrary units; normalized to average of uninfected parenchyma = 1; mean ± SE; n = 5 mice per group; ANOVA on ranks P=0.008; *P<0.05 by post-hoc Dunn's test). (**G**) Mean fluorescent intensity of TGF-β1+ pixels (arbitrary units; normalized to average of uninfected parenchyma = 1; mean ± SE; n = 5 mice per group; ANOVA on ranks P=0.005; *P<0.05 by post-hoc Dunn's test). (**H**) Ratio of areas of co-localized Mac3+ and TGF-β1+ area to all TGF-β1+ area in the parenchyma and peri-egg granulomas (mean ± SE; n = 5 mice per group; ANOVA on ranks P=0.005; *: P<0.05 by post-hoc Dunn's test).

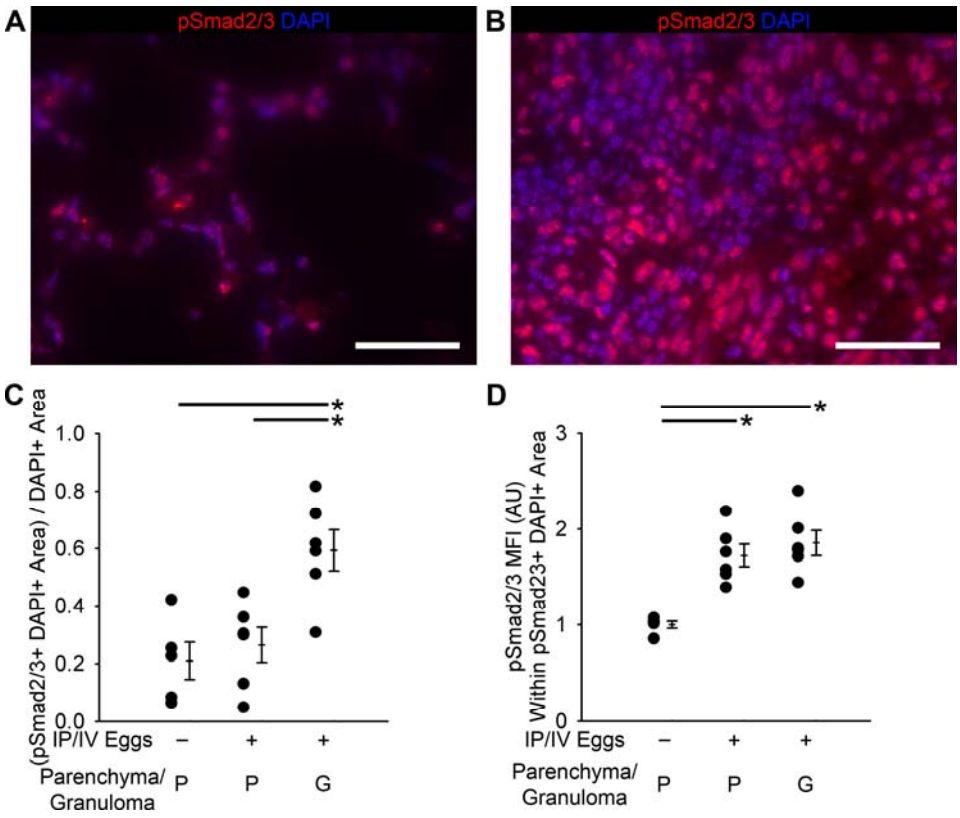

Figure S12.
Quantification of phospho-Smad2/3 quantity and co-localization with parenchyma and peri-egg granuloma compartments in unexposed and mice exposed to IP and IV *S. mansoni* eggs. (**A**) Representative image showing phospho-Smad2/3 in the parenchyma of an IP/IV *S. mansoni* egg-exposed mouse (Scale bars: 50 μm). (**B**) Representative image showing phospho-Smad2/3 in the peri-egg granuloma of an IP/IV *S. mansoni* egg-exposed mouse (Scale bars: 50 μm). (**C**) Quantification of phospho-Smad2/3+ area in the parenchyma and granuloma (mean ± SE; n = 5 mice per group; ANOVA on ranks P=0.009; *P<0.05 by post-hoc Dunn's test). (**D**) Mean fluorescent intensity of phospho-Smad2/3+ pixels in the parenchyma and granuloma (arbitrary units; normalized to average of uninfected parenchyma = 1; mean ± SE; n = 5 mice per group; ANOVA on ranks P=0.007; *P<0.05 by post-hoc Dunn's test).

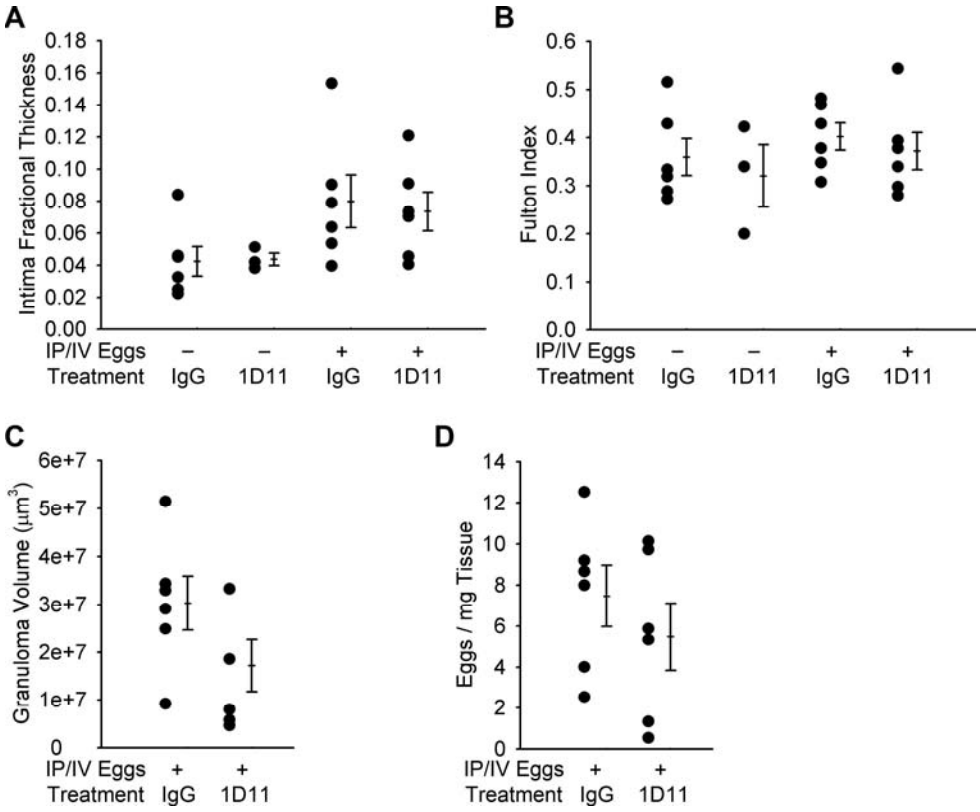

Figure S13.
Exposure to 1D11 does not affect intima thickness, RV hypertrophy, per-egg granuloma volumes or eggs cleared from the lung tissue. (**A**) Quantitative intima fractional thickness (mean ± SE; n = 3-6 mice per group; ANOVA on ranks *P*=0.087). (**B**) Fulton index (mean ± SE; n = 3-6 mice per group; ANOVA on ranks *P*=0.56). (**C**) Peri-egg granuloma volume (mean ± SE; n = 3-6 mice per group; rank-sum test *P*=0.18). (**D**) Egg counts after 4% KOH digest (mean ± SE; n = 3-6 mice per group; rank-sum test *P*=0.59).

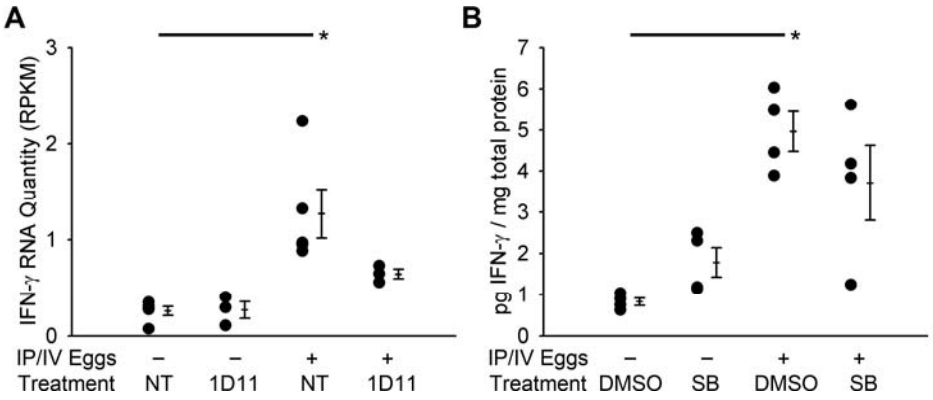

Figure S14.
Effect of 1D11 on IFN-γ levels. (**A** and **B**) IFN-γ RNA and protein quantity as measured by RNA-seq and ELISA in mice treated with SB431542, 1D11, DMSO, or no treatment (NT), unexposed or IP/IV exposed to *S. mansoni* eggs (mean ± SE; n = 3-5 mice per group; ANOVA on ranks P=0.005 for RNA data, P=0.007 for protein data; *P<0.05 by post-hoc Dunn's test).

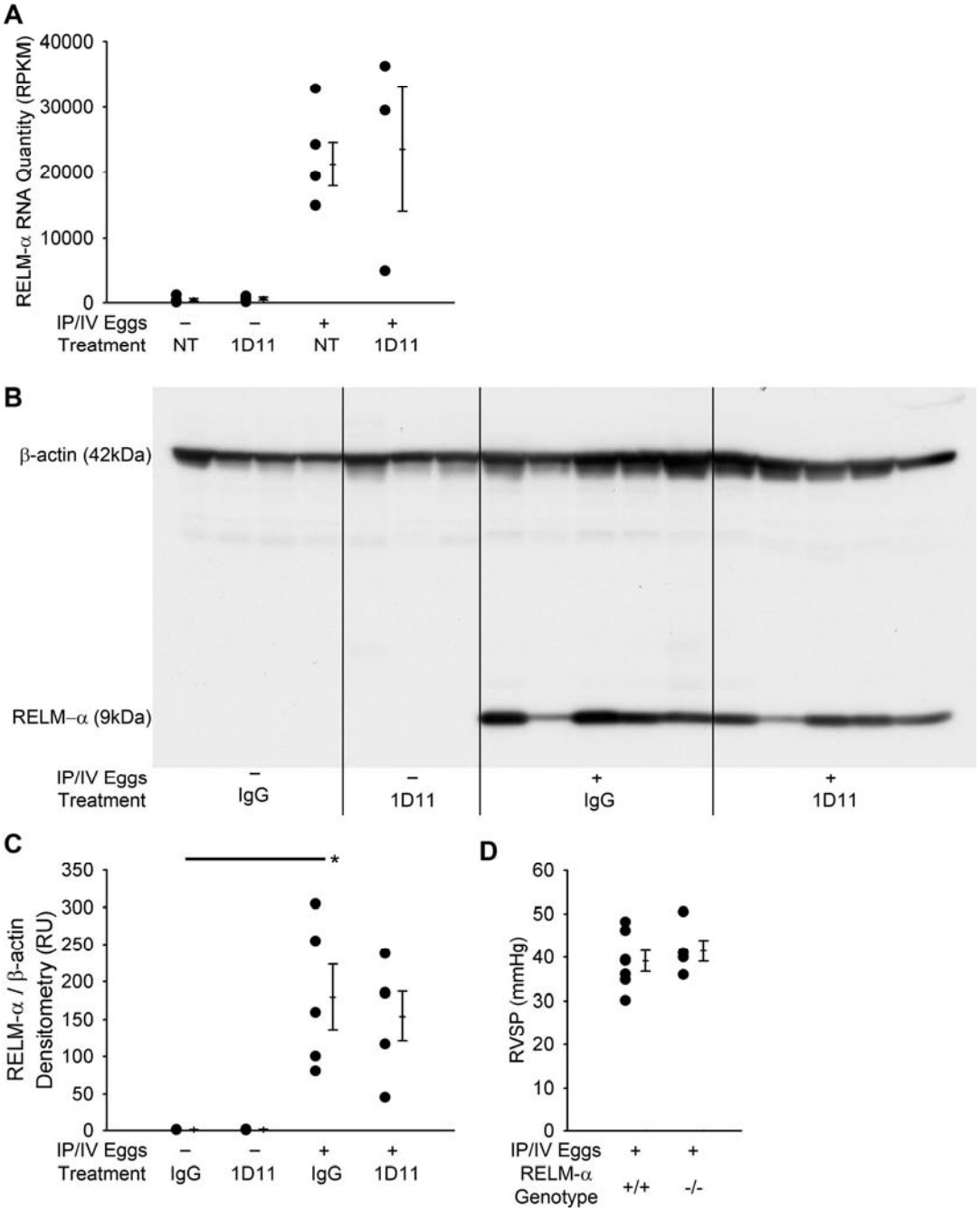

Figure S15.
Effect of TGF-β signaling blockade on RELM-α. (**A**) RELM-α RNA quantity as measured by RNA-seq in mice treated with 1D11 or no treatment (NT), unexposed or IP/IV exposed to *S. mansoni* eggs (RPKM: reads per kilobase of exon model per million mapped reads; mean ± SE; n = 3-5 mice per group; ANOVA on ranks P=0.010). (**B** and **C**) Western blot and densitometry quantification of whole lung lysates from mice treated with 1D11 or IgG, unexposed or IP/IV exposed to *S. mansoni* eggs, and probed for RELM-α and β-actin (relative units; ratio normalized to average of unexposed IgG treated = 1; mean ± SE; n = 3-5 mice per group; ANOVA on ranks P=0.008; *P<0.05 by post-hoc Dunn's test). (**D**) RVSP in RELM-α+/+ and

RELM-α-/- mice (both on a Balb-c background) IP/IV exposed to *S. mansoni* eggs (mean ± SE; n = 5-7 mice per group; rank-sum test *P*=0.34).

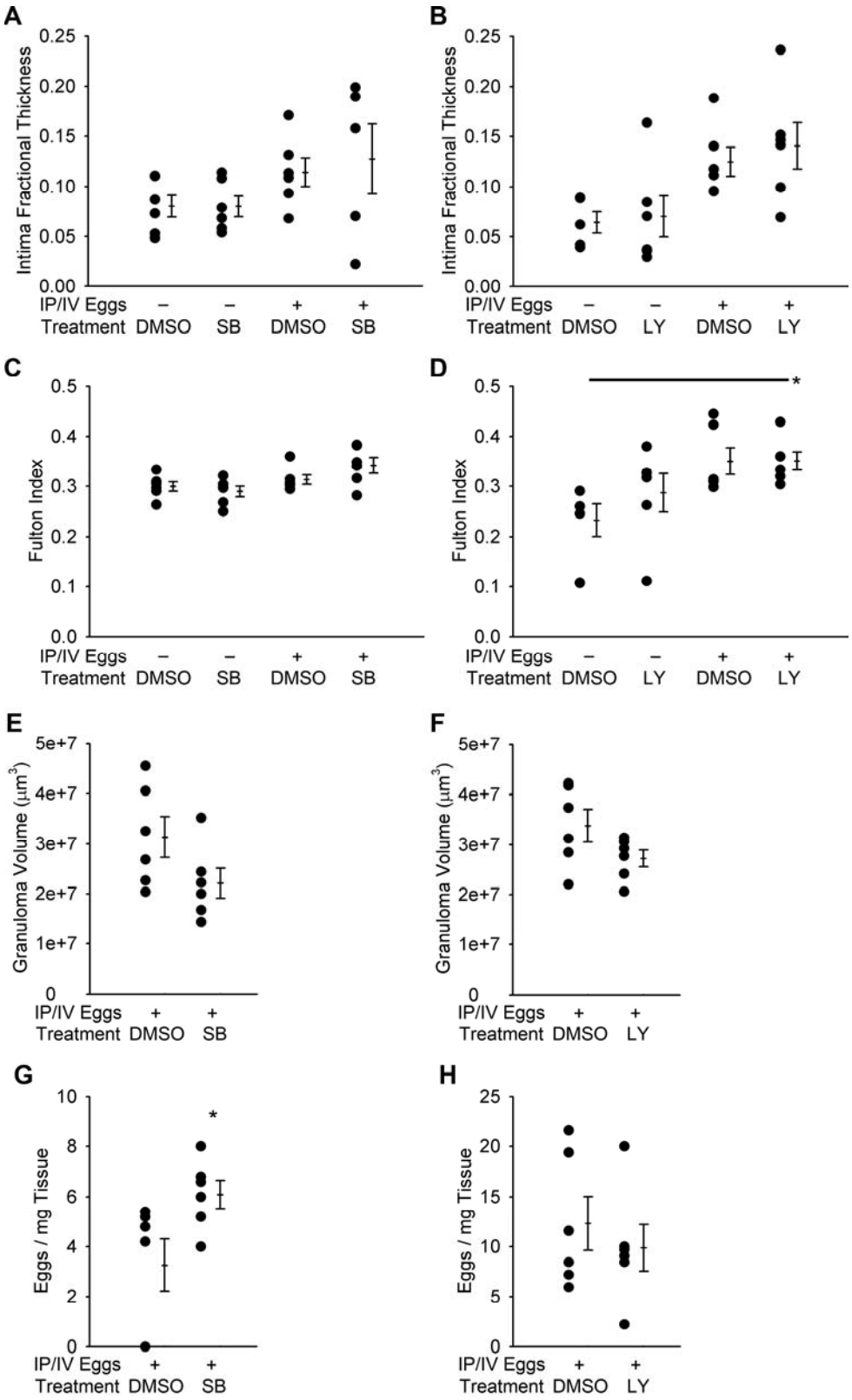
A
Intima Fractional Thickness
0.25
0.20
0.15
0.10
0.05
0.00
IP/IV Eggs – – + +
Treatment DMSO SB DMSO SB
B
Intima Fractional Thickness
0.25
0.20
0.15
0.10
0.05
0.00
IP/IV Eggs – – + +
Treatment DMSO LY DMSO LY
C
Fulton Index
0.5
0.4
0.3
0.2
0.1
0.0
IP/IV Eggs – – + +
Treatment DMSO SB DMSO SB
D
Fulton Index
*
0.5
0.4
0.3
0.2
0.1
0.0
IP/IV Eggs – – + +
Treatment DMSO LY DMSO LY
E
Granuloma Volume (μm3)
5e+7
4e+7
3e+7
2e+7
1e+7
0
IP/IV Eggs + +
Treatment DMSO SB
F
Granuloma Volume (μm3)
5e+7
4e+7
3e+7
2e+7
1e+7
0
IP/IV Eggs + +
Treatment DMSO LY
G
Eggs / mg Tissue
*
10
8
6
4
2
0
IP/IV Eggs + +
Treatment DMSO SB
H
Eggs / mg Tissue
25
20
15
10
5
0
IP/IV Eggs + +
Treatment DMSO LY

Figure S16.

Treatment with either of two TGF-β receptor type 1 (ALK5) inhibitors SB431542 or LY364947 prevents the increase in pressure from IP/IV egg exposure. (**A**-**B**) Quantitative fractional thickness of the pulmonary vascular intima in mice treated with SB431542, LY364947 or DMSO vehicle, and unexposed or IP/IV exposed to *S. mansoni* eggs (mean ± SE; n = 5-6 mice per group; ANOVA on ranks *P*=0.303 for SB431542 treatment, *P*=0.016 for LY364947 treatment). (**C**-**D**) Fulton index (mean ± SE; n = 5-6 mice per group; ANOVA *P*=0.018 for SB431542 treatment; ANOVA *P*=0.017 for LY364947 treatment; **P* < 0.05 by post-hoc Tukey test). (**E**-**F**) Granuloma volume (mean ± SE; n = 5-6 mice per group; rank-sum test *P*=0.093 for SB431542 treatment, *P*=0.18 for LY364947 treatment). (**G**-**H**) Egg counts after 4% KOH digest (mean ± SE; n = 5-6 mice per group; rank-sum test **P*<0.05 for SB531542 treatment, *P*=0.82 for LY364947 treatment).

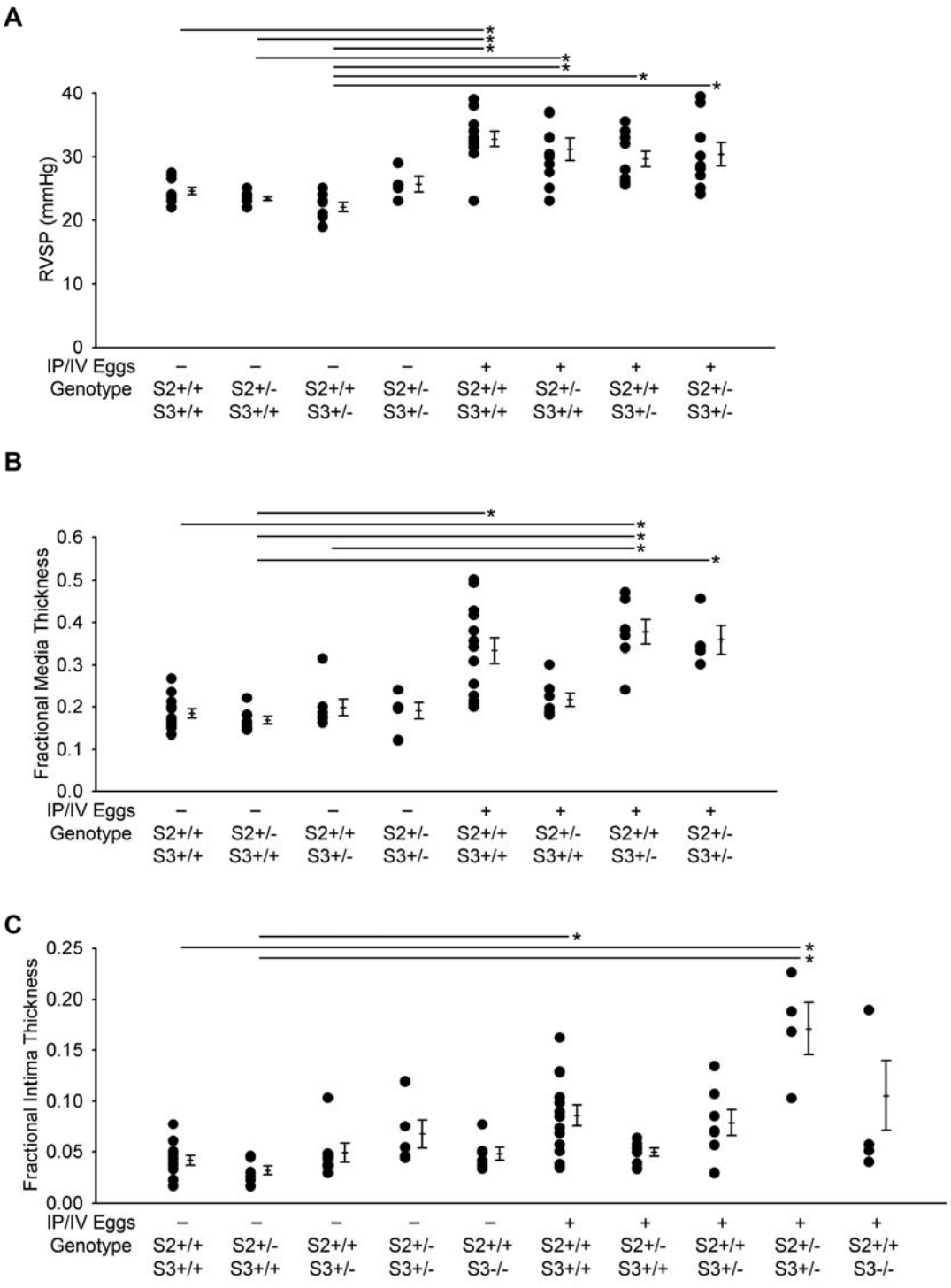

Figure S17 (Continued on next page).

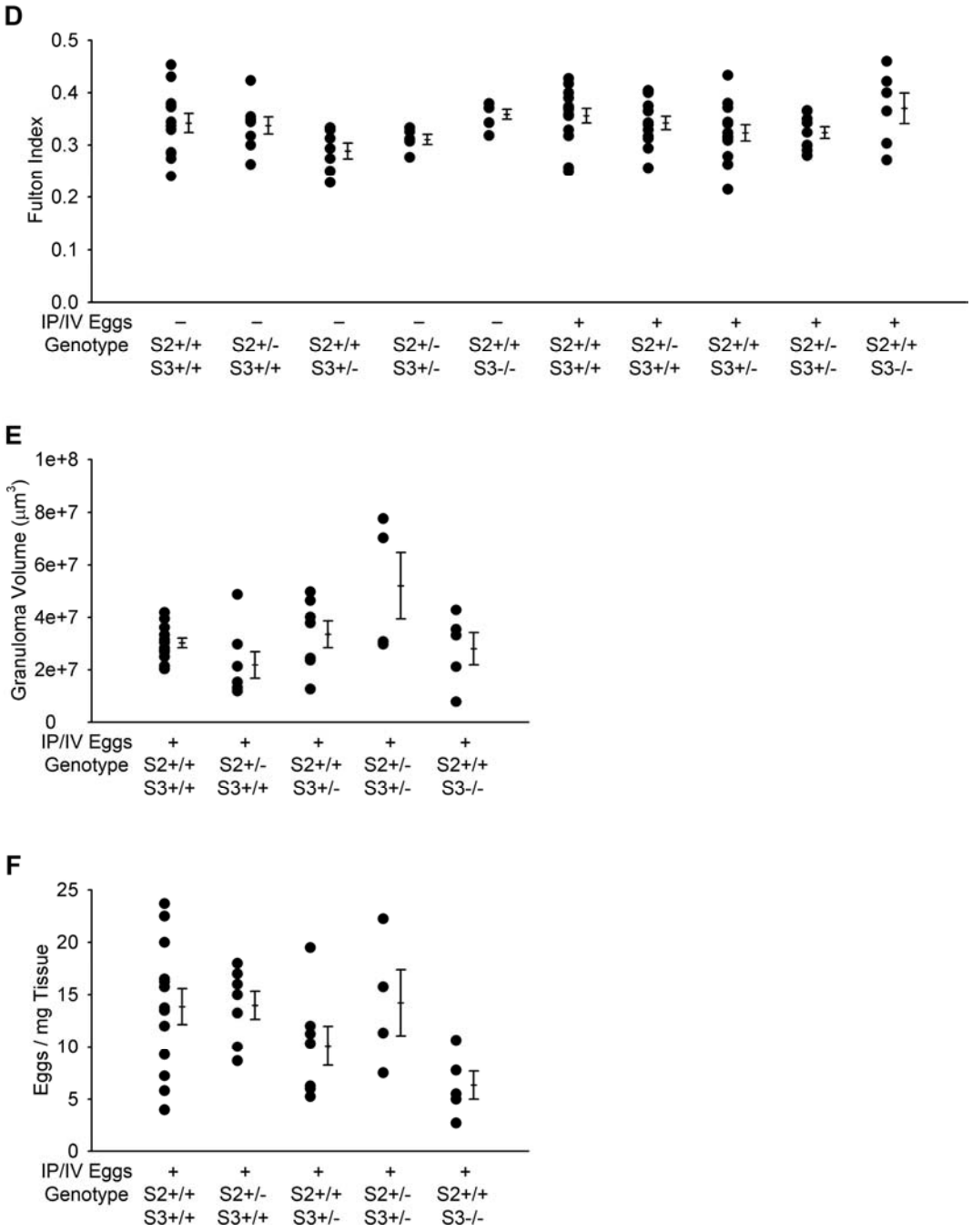

Figure S17.
Smad2+/-, Smad3+/-, Smad2+/-Smad3+/- and Smad3-/- genotypes with IP/IV egg exposure. (**A**) RVSP in wildtype, Smad2+/-, Smad3+/- and Smad2+/-Smad3+/- mice unexposed or IP/IV exposed to *S. mansoni* eggs (mean ± SE; n = 4-12 mice per group (note data for 6 wildtype uninfected and 6 wildtype infected mice presented in Figure 11A are also included ; ANOVA on ranks $P<0.001$; *$P < 0.05$ by post-hoc Dunn's test). (**B**) Quantitative fractional thickness of the pulmonary vascular media in wildtype, Smad2+/-, Smad3+/- and Smad2+/-Smad3+/- mice unexposed or IP/IV exposed to *S. mansoni* eggs (mean ± SE; n = 4-13 mice per group; note data for 6 wildtype uninfected and 6 wildtype infected mice presented in Figure 11A are also included; ANOVA on ranks $P<0.001$; *$P < 0.05$ by post-hoc Dunn's test). (**C**) Quantitative

fractional thickness of the pulmonary vascular media in wildtype, Smad2+/-, Smad3+/-, Smad2+/-Smad3+/- and Smad3-/- mice unexposed or IP/IV exposed to *S. mansoni* eggs (mean ± SE; n = 4-13 mice per group; ANOVA on ranks $P<0.001$; *$P < 0.05$ by post-hoc Dunn's test). (**D**) Fulton index in wildtype, Smad2+/-, Smad3+/-, Smad2+/-Smad3+/- and Smad3-/- mice unexposed or IP/IV exposed to *S. mansoni* eggs (mean ± SE; n = 5-13 mice per group; ANOVA on ranks $P=0.070$).(**E**) Granuloma volume in wildtype, Smad2+/-, Smad3+/-, Smad2+/-Smad3+/- and Smad3-/- mice unexposed or IP/IV exposed to *S. mansoni* eggs (mean ± SE; n = 4-13 mice per group; ANOVA on ranks $P=0.16$). (**F**) Egg counts after 4% KOH digest in wildtype, Smad2+/-, Smad3+/-, Smad2+/-Smad3+/- and Smad3-/- mice unexposed or IP/IV exposed to *S. mansoni* eggs (mean ± SE; n = 4-13 mice per group; ANOVA on ranks $P=0.053$).

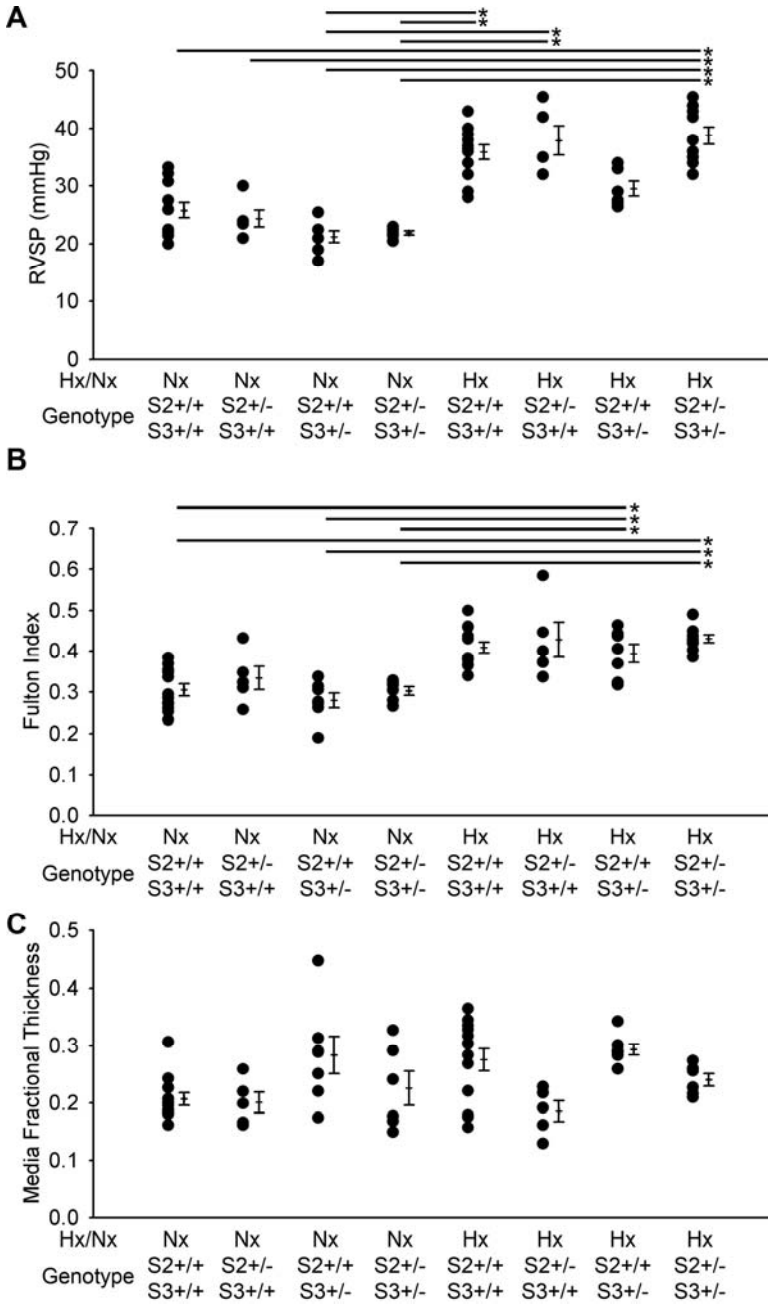

Figure S18 (Continued on next page).

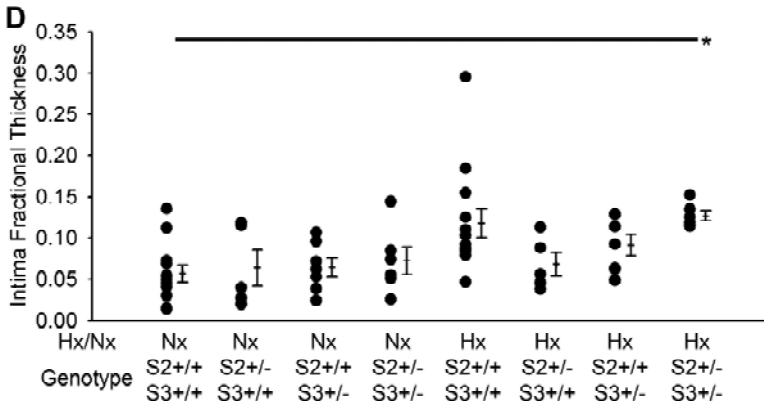

Figure S18.
Effect of Smad2+/- and Smad3+/- genotypes on hypoxia-induced pulmonary hypertension. (**A**) RVSP (mean ± SE; n = 5-12 mice per group; ANOVA on ranks $P<0.001$; *$P < 0.05$ by post-hoc Dunn's test). (**B**) Fulton index (mean ± SE; n = 5-13 mice per group; ANOVA on ranks $P<0.001$; *$P < 0.05$ by post-hoc Dunn's test). (**C** and **D**) Quantitative fractional thickness of the pulmonary vascular media and intima (mean ± SE; n = 5-13 mice per group; ANOVA on ranks $P=0.006$ for media, $P=0.004$ for intima; *$P < 0.05$ by post-hoc Dunn's test).

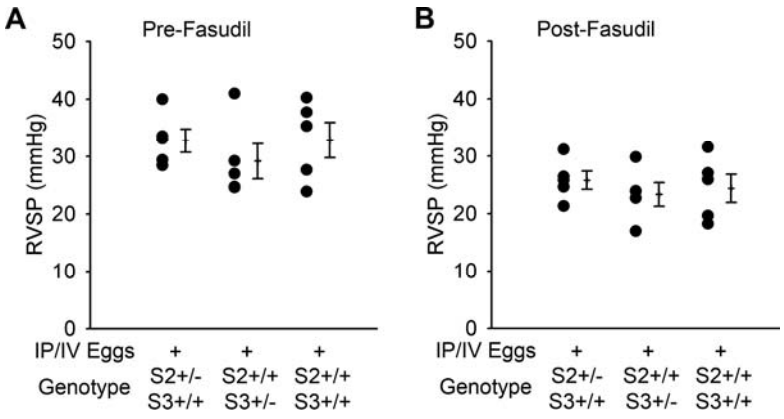

Figure S19.
Effect of the Rho kinase inhibitor fasudil in mice lacking Smad2 and/or Smad3. (**A** and **B**) RVSP in unexposed and IP/IV egg exposed Smad2+/-, Smad3+/-, and Smad2+/-Smad3+/- mice before and 5 minutes after acute fasudil administration (mean ± SE; n = 5-6 mice per group; ANOVA on ranks *P*=0.53 for pre-fasudil, *P*=0.60 for post-fasudil). The decrease in pressure is shown in **Figure 8G**.

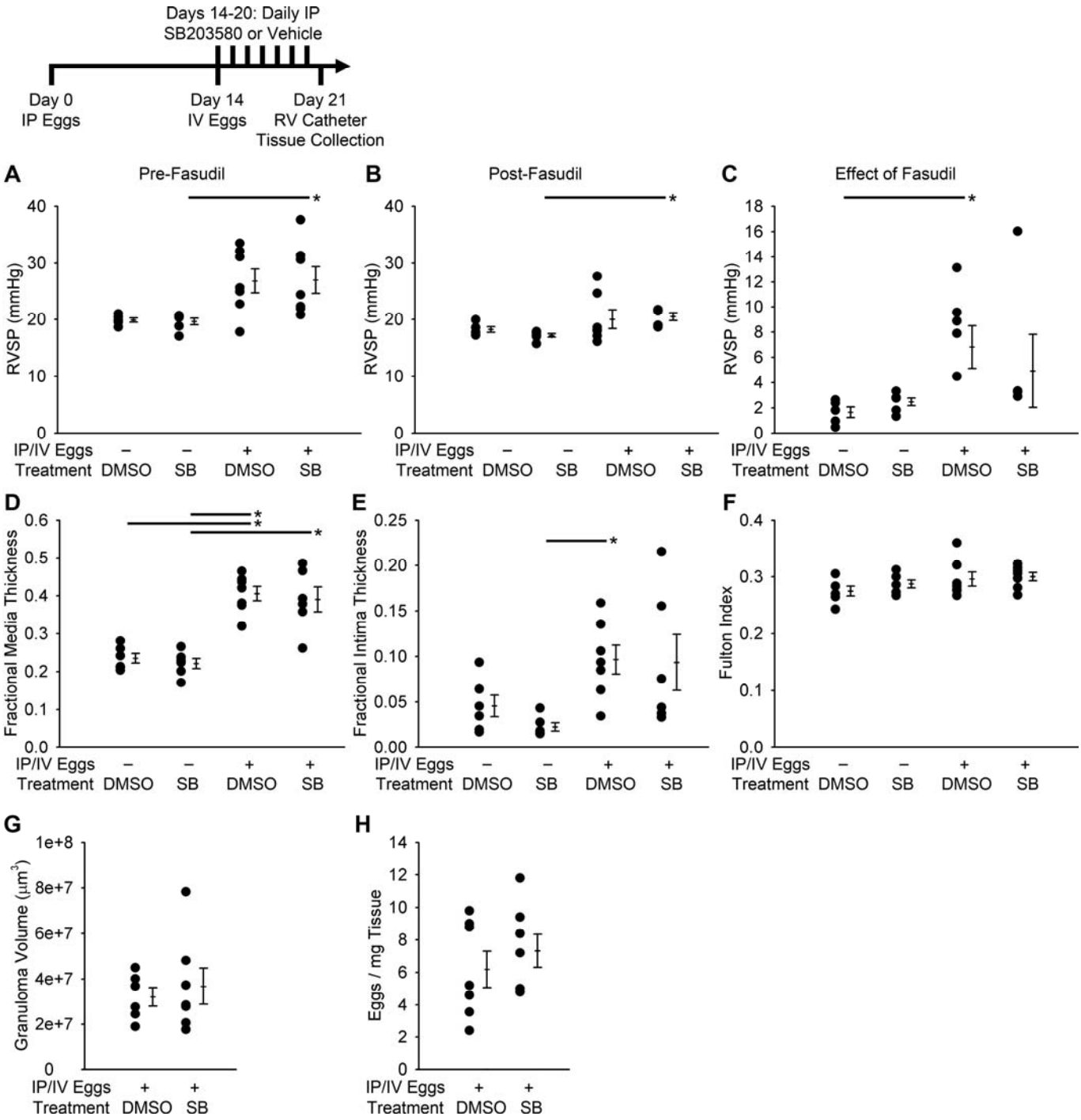

Figure S20.
Treatment with the p38 kinase inhibitor SB203580 has no additional effect on *S. mansoni*–induced pulmonary hypertension. (**A**-**C**) RVSP in unexposed and IP/IV egg exposed mice treated with SB203580 or vehicle control, before and after fasudil administration, and the decrease in pressure (mean ± SE; n = 5-7 mice per group; ANOVA on ranks P=0.005 for pre-fasudil, P=0.024 for post-fasudil, P=0.038 for change in pressure; *P < 0.05 by post-hoc Dunn's test). (**D** and **E**) Quantitative fractional thickness of the pulmonary vascular media and intima (mean ± SE; n = 6-7 mice per group; ANOVA on ranks P<0.001 for media, P=0.007 for intima;

*$P < 0.05$ by post-hoc Dunn's test). (**F**) Fulton index (mean ± SE; n = 6-7 mice per group; ANOVA on ranks $P=0.24$). (**G**) Peri-egg granuloma volume (mean ± SE; n = 6-7 mice per group; rank-sum test $P=0.84$). (**H**) Egg counts after 4% KOH digest (mean ± SE; n = 7 mice per group; rank-sum test $P=0.54$).

Supplemental References

(1) Cheever AW. Conditions affecting the accuracy of potassium hydroxide digestion techniques for counting Schistosoma mansoni eggs in tissues. *Bull World Health Organ*. 1968;39:328-31.

(2) Graham BB, Mentink-Kane MM, El-Haddad H, Purnell S, Zhang L, Zaiman A, Redente EF, Riches DW, Hassoun PM, Bandeira A, Champion HC, Butrous G, Wynn TA, Tuder RM. Schistosomiasis-induced experimental pulmonary hypertension: role of interleukin-13 signaling. *Am J Pathol*. 2010;177:1549-61.

(3) Tandrup T, Gundersen HJ, Jensen EB. The optical rotator. *J Microsc*. 1997;186:108-20.